

The Role of Weakly Bound On-Top Oxygen in the Catalytic CO Oxidation Reaction over RuO₂(110)

Stefan Wendt,^{†,‡} Marcus Knapp,[†] and Herbert Over^{*,†}

Contribution from the Department of Physical Chemistry, Justus-Liebig-University, Heinrich-Buff-Ring 58, D-35392 Giessen, Germany, and Department of Physical Chemistry, Fritz-Haber-Institut der Max-Planck-Gesellschaft, Faradayweg 4-6, D-14195 Berlin, Germany

Received May 30, 2003; E-mail: herbert.over@phys.chemie.uni-giessen.de

Abstract: RuO₂-based catalysts are much more active in the oxidation of CO than related metallic Ru catalysts. This high catalytic activity (or low activation barrier) is attributed to the weak oxygen surface bonding of bridging O atoms on RuO₂(110) in comparison with the strongly chemisorbed oxygen on Ru(0001). Since the RuO₂(110) surface is able to stabilize an even more weakly bound on-top oxygen species, one would anticipate that the catalytic activity will increase further under oxidizing conditions. We will show that this view is far too simple to explain our temperature-programmed reaction experiments, employing isotope labeling of the potentially active surface oxygen species on RuO₂(110). Rather, both surface O species on RuO₂(110) reveal similar activities in oxidizing CO.

1. Introduction

In general, the catalytic activity for the CO oxidation over transition-metal surfaces is determined by the propensity of the metal surface to dissociate oxygen molecules and is counter balanced by the bond strength of the active oxygen species on the surface.¹ Accordingly, transition metals with half-filled d-bands, where the dissociation probability is not too low and the adsorption energy of oxygen is not too high, reveal the highest activity. The activation barrier of the catalyzed CO oxidation reaction over transition-metal surfaces is considered to be determined by the metal–oxygen bond breaking.²

A particularly interesting system is encountered with the CO oxidation over ruthenium (Ru). Metallic Ru is a poor catalyst for the oxidation of CO under ultrahigh vacuum (UHV) conditions due to the high binding energy of chemisorbed oxygen.^{3,4} However, metallic Ru turns into a very efficient oxidation catalyst under high pressures and oxidizing conditions.^{4–9} The reason for this dramatic enhancement in the catalytic activity has been identified with the structural transformation of the metallic Ru into the oxide RuO₂.⁷ To a first

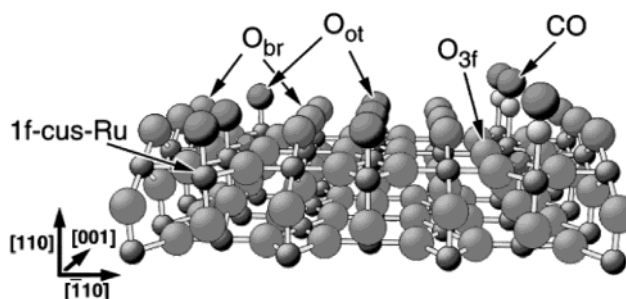


Figure 1. Ball and stick model of the RuO₂(110) surface, which is covered by on-top O (O_{ot}) and on-top CO. Large balls represent oxygen, and small balls represent ruthenium atoms of RuO₂(110). The bridge-bonded O species (O_{br}), the 3-fold-coordinated O species (O_{3f}), the CO molecule (CO), the 1-fold undercoordinated Ru (1f-cus-Ru), and the on-top bonded oxygen (O_{ot}) are indicated.

approximation, the high activity of RuO₂ was traced back to the low binding energy of the bridging O atoms⁷ (cf. O_{br} in Figure 1) together with a high dissociative sticking probability of oxygen on RuO₂.¹⁰

Under reaction conditions, a well-defined RuO₂(110) surface—serving as a model catalyst for RuO₂—offers two potentially active oxygen species, namely the bridging O atoms (O_{br}) and the on-top oxygen species (O_{ot}) (cf. Figure 1). The adsorption energy of O_{ot} is lower (by 1.4 eV) than that of the O_{br} atoms.¹¹ According to the Brønsted–Evans–Polanyi (BEP) type relationship,¹² the activation energy will be lower the greater the thermodynamic driving force for a reaction is. Therefore, the O_{ot} species on RuO₂(110) is anticipated to be much more active in oxidizing CO than the O_{br} atoms, a conclusion that was

[†] Justus-Liebig-University.

[‡] Fritz-Haber-Institut der Max-Planck-Gesellschaft.

- (1) *Handbook of Heterogeneous Catalysis*; Ertl, G., Knözinger, H., Weitkamp, J., Eds.; Wiley: New York, 1997; Vol. 5.
- (2) Peden, C. H. F. In *Surface Science of Catalysis*, Dwyer, D. J., Hoffmann, F. M., Eds.; ACS Symposium Series 483; American Chemical Society: Washington, DC, 1992; p 143.
- (3) (a) Lee, H.-I.; White, J. M. *J. Catal.* **1980**, *63*, 261. (b) Savchenko, V. I.; Borezkov, G. K.; Kalinkin, A. V.; Salanow, A. N. *Kinet. Katal.* **1984**, *24*, 983.
- (4) Peden, C. H. F.; Goodman, D. W. *J. Phys. Chem.* **1986**, *90*, 1360.
- (5) Böttcher, A.; Rogazia, M.; Niehus, H.; Over, H.; Ertl, G. *J. Phys. Chem. B* **1999**, *103*, 6267.
- (6) Zang, L.; Kisch, H. *Angew. Chem., Int. Ed.* **2000**, *39*, 3921.
- (7) Over, H.; Kim, Y. D.; Seitsonen, A. P.; Wendt, S.; Lundgren, E.; Schmid, M.; Varga, P.; Morgante, A.; Ertl, G. *Science* **2000**, *287*, 1474.
- (8) Kim, Y. D.; Over, H.; Krabbes, G.; Ertl, G. *Top. Catal.* **2001**, *14*, 95.
- (9) Over, H.; Muhler, M. *Prog. Surf. Sci.* **2003**, *72*, 3.

(10) Böttcher, A.; Niehus, H. *Phys. Rev. B* **1999**, *60*, 14396.

(11) Kim, Y. D.; Seitsonen, A. P.; Wendt, S.; Wang, J.; Fan, C. Y.; Jacobi, K.; Over, H.; Ertl, G. *J. Phys. Chem. B* **2001**, *105*, 3752.

(12) (a) Brønsted, N. *Chem. Rev.* **1928**, *5*, 231. (b) Evans, M. G.; Polanyi, N. P. *Trans. Faraday Soc.* **1936**, *32*, 1333.

apparently supported by a recent high-resolution electron energy-loss spectroscopy (HREELS) study.¹³

In this paper, we provide experimental evidence that the O_{ot} species is not more active in oxidizing CO than the O_{br} species. We performed temperature-programmed desorption and reaction (TPD/TPR) experiments for various precoverages of the O_{ot} species. To disentangle contributions in TPR coming from the recombination of CO with O_{br} and O_{ot} , we labeled the O_{ot} species with ^{18}O .

2. Experimental Details and Properties of $RuO_2(110)$

The TPD/TPR experiments were conducted in an UHV chamber equipped with low-energy electron diffraction (SPA-LEED) optics, a quadrupole mass spectrometer (QMS), and facilities for surface preparation and cleaning. The differentially pumped QMS was connected to the main chamber via a closed cone with a small aperture ($d = 2.5$ mm) facing the sample at a distance of 1 mm. This ensured that only molecules released from the sample could reach the QMS. The $Ru(0001)$ sample was clamped between two tungsten wires. The temperature of the sample could be varied from 140 K (by cooling with liquid N_2) to 1530 K (by direct resistive heating). The sample temperature was measured by a Ni/NiCr thermocouple which was spot-welded to the backside of the sample.

The $Ru(0001)$ sample was cleaned by argon ion bombardment at 1 keV, followed by cycles of oxygen exposure at 1000 K to remove surface carbon. Final traces of oxygen were removed by flashing the surface to 1530 K, resulting in a sharp (1×1) LEED pattern.

The ultrathin $RuO_2(110)$ film was produced by exposing a well-prepared single-crystal $Ru(0001)$ to high doses of oxygen ($^{16}O_2$) at a sample temperature of 750 K.¹⁴ A typical oxygen dose for producing the $RuO_2(110)$ film is 6×10^{16} Langmuirs (L); (1 L = 1.33×10^{-6} mbar·s). A glass capillary array was used to dose such high amounts of oxygen. The local oxygen pressure in front of the sample was estimated to be about 1×10^{-2} mbar while the background pressure did not exceed 1×10^{-4} mbar. After the background pressure in the UHV chamber had reached a value below 10^{-9} mbar, the contamination by residual oxygen adsorption was removed by briefly heating the sample to 600 K.

RuO_2 crystallizes in the rutile structure. The $RuO_2(110)$ surface exposes two kinds of undercoordinated surface atoms (cf. Figure 1), namely the bridging oxygen atoms O_{br} , which are coordinated only to two Ru atoms underneath, and the so-called 1f-cus-Ru atoms, i.e., 1-fold coordinatively unsaturated Ru sites.¹⁴

CO adsorption on the bare $RuO_2(110)$ surface proceeds via the 1f-cus-Ru atoms in terminal position (cf. Figure 1). At temperatures below 200 K, the on-top CO species is stable on the surface (the binding energy was 1.2 eV).¹⁵ At higher temperatures, say at room temperature (RT) and above, the CO molecules recombines with neighboring O_{br} atoms to form CO_2 ,¹³ thereby creating vacancies in the rows of O_{br} atoms.¹⁶

We prepared the pristine $RuO_2(110)$ film exclusively with $^{16}O_2$, while the O_{ot} species was isotope labeled by dosing $^{18}O_2$ at RT. We checked carefully the purity of the $^{18}O_2$ input (the bottle contained less than 3% $^{16}O_2$). Control experiments showed that exchange reactions of ^{18}O with ^{16}O at the chamber wall were negligible. After each TPD/TPR experiment, the $RuO_2(110)$ surface was exposed to ca. 20 L of oxygen $^{16}O_2$ at 750 K to restore a stoichiometric surface with ^{16}O atoms on all bridging positions. For the TPD and TPR experiments, the heating rate was 4.5 K/s.

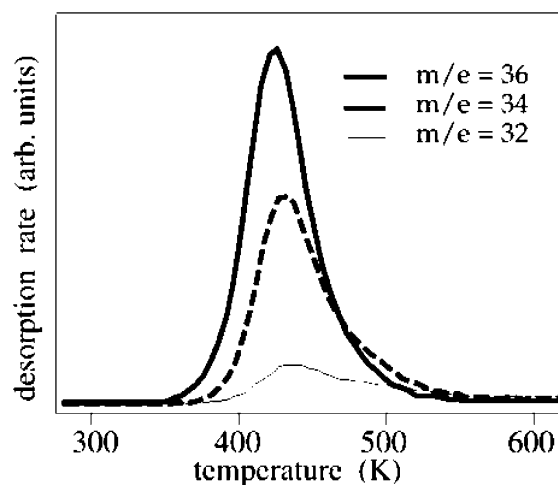


Figure 2. Thermal desorption spectra of on-top oxygen on $RuO_2(110)$. The clean $RuO_2(110)$ surface was produced with $^{16}O_2$, while the O_{ot} species was labeled by $^{18}O_2$. The thermal desorption spectra for $m/e = 32, 34$, and 36 are taken after the clean $RuO_2(110)$ surface was saturated with 2 L $^{18}O_2$ at RT.

3. Isotope Labeling Experiments

3.1. Complex Interaction of the Weakly Bound On-Top O Species with $RuO_2(110)$. Exposing the $RuO_2(110)$ surface to a few Langmuirs of $^{18}O_2$ at RT produced a weakly bound oxygen species¹⁰ which adsorbs directly above the 1f-cus-Ru atom in terminal position (cf. O_{ot} in Figure 1)¹¹ and desorbs completely at 430 K.¹⁰ All other O atoms of $RuO_2(110)$ were labeled by ^{16}O . In Figure 2 we took simultaneously the thermal desorption spectra for $m/e = 32, 34$, and 36 ; these were the atomic mass units for molecular oxygen consisting of two ^{16}O , a mixture of ^{16}O and ^{18}O , or two ^{18}O atoms, respectively. The integrated intensities of the mixed state ($m/e = 34$) and the $m/e = 32$ signal were about 60% and 10% of that of the $m/e = 36$ signal, respectively.

One way to explain the $m/e = 34$ spectrum in Figure 2 is that $^{16}O_{br}$ and $^{18}O_{ot}$ directly recombined to form O_2 . However, the binding energy difference between O_{br} and O_{ot} is as high as 1.4 eV,¹¹ and therefore, a direct recombination of O_{br} and O_{ot} should have occurred only above 650 K rather than around 430 K. Also, since the oxygen desorption traces in Figure 2 were very much alike (in particular, the maximum desorption rate was at about 430 K for all oxygen masses), the $^{16}O + ^{18}O$ and the $^{16}O + ^{16}O$ signals both originated from the association of neighboring O_{ot} atoms. Consequently, an exchange reaction between O_{ot} and another surface oxygen species had to precede the actual recombination step. From an energetical point of view, an exchange reaction of O_{ot} atoms with lattice O_{3f} atoms was much less favorable (the energy difference was 2.6 eV¹¹) than an exchange between O_{ot} and O_{br} (energy difference was 1.4 eV¹¹). From the integrated intensity of the $m/e = 36, 34$, and 32 TPD/TPR spectra in Figure 2, we estimated that about 25% of the O_{br} and O_{ot} atoms had exchanged. Our TPD/TPR data are largely consistent with recent experiments of Böttcher et al.,¹⁷ although their interpretation in terms of a transformation of adsorbed oxygen into subsurface oxygen is untenable. Böttcher et al. determined an exchange ratio of 20% (cf. η in Figure 4 of ref 17), which is in nice agreement with our estimation of 25%.

(13) Fan, C. Y.; Wang, J.; Jacobi, K.; Ertl, G. *J. Chem. Phys.* **2001**, *114*, 10058.

(14) Kim, Y. D.; Seitsonen, A. P.; Over, H. *Surf. Sci.* **2000**, *465*, 1.

(15) Kim, Y. D.; Seitsonen, A. P.; Over, H. *Phys. Rev. B* **2001**, *63*, 115419.

(16) Over, H.; Seitsonen, A. P.; Lundgren, E.; Schmid, M.; Varga, P. *J. Am. Chem. Soc.* **2001**, *123*, 11807.

(17) Böttcher, A.; Conrad, H.; Niehus, H. *Surf. Sci.* **2001**, *478*, 229.

Next, we prepared the on-top ^{18}O -covered $\text{RuO}_2(110)$ surfaces at various sample temperatures (275, 300, 325, and 350 K) to identify the temperature range where O_{br} and O_{ot} started to exchange. It turned out that the amount of exchanged oxygen atoms did not change for the various preparation temperatures up to 350 K, consistent with recent experiments of Böttcher et al. (cf. Figure 2 in ref 17). Accordingly, the $\text{O}_{\text{ot}}/\text{O}_{\text{br}}$ exchange reaction proceeded at temperatures higher than 350 K. On the other hand, 25% of the O_{br} and O_{ot} did exchange during the desorption process. Therefore, the $m/e = 34$ curve in Figure 2 may be considered as a convolution of the $m/e = 36$ signal (pure recombination: second-order kinetics) and an Arrhenius-like function $A \cdot \exp(-\Delta E_x/kT)$, approximating the activated exchange process (ΔE_x : activation energy); typical values for the frequency factor A are in the range of 10^{10} to 10^{15} . As a result of the convolution, the $m/e = 34$ spectrum becomes asymmetric, intersecting the $m/e = 36$ trace at about 475 K, and the maximum shifts to higher temperatures consistent with our measurements. The $m/e = 32$ signal required two exchange processes per desorbing oxygen molecule so that the $m/e = 32$ curve should have been even more asymmetric than the $m/e = 34$ spectrum as seen indeed in Figure 2. With the frequency factor to be in the range 10^{10} to 10^{13} we estimated an activation energy of 0.8–1.1 eV for the $\text{O}_{\text{ot}}/\text{O}_{\text{br}}$ exchange reaction.

Recently, a similar exchange process had been identified with the diffusion of O_{br} vacancy on the rutile $\text{TiO}_2(110)$ surface, using high-resolution, fast-scanning STM.¹⁸ This diffusion process was mediated by a complex reaction with adsorbed molecular oxygen, where one of the oxygen atoms of the O_2 molecule exchanged with O_{br} .

3.2. TPR Measurements of the CO Oxidation Reaction over the On-Top Oxygen Precovered $\text{RuO}_2(110)$ Surface. The various precoverages of on-top ^{18}O were prepared by directly exposing specific doses of $^{18}\text{O}_2$ at RT, i.e., far below the temperature where $\text{O}_{\text{ot}}/\text{O}_{\text{br}}$ exchange takes place. Subsequently, the partly $^{18}\text{O}_{\text{ot}}$ precovered surface was saturated with $^{12}\text{C}^{16}\text{O}$ at 170 K. This procedure ensured that all 1f-cus-Ru atoms were capped by either CO or $^{18}\text{O}_{\text{ot}}$ with a varying ratio of absorbed CO and O_{ot} . The O_{br} atoms were labeled with the isotope ^{16}O .

In Figure 3a, we present CO_2 TPR spectra for $m/e = 44$ ($^{16}\text{O}^{12}\text{C}^{16}\text{O}$) and $m/e = 46$ ($^{16}\text{O}^{12}\text{C}^{18}\text{O}$) of a $\text{RuO}_2(110)$ surface which was preexposed to 0.2 L $^{18}\text{O}_2$. After subsequent CO saturation, such a surface was covered with 0.2 monolayers (ML) of on-top ^{18}O and with 0.8 ML of CO. Upon heating the sample to 600 K, two times more CO_2 of $m/e = 44$ ($^{16}\text{O}^{12}\text{C}^{16}\text{O}$) was produced than CO_2 of $m/e = 46$ ($^{16}\text{O}^{12}\text{C}^{18}\text{O}$). However, we should keep in mind that the O_{ot} coverage was by a factor of 5 smaller than the O_{br} coverage. The shapes of the TD traces in Figure 3 (upper panel) are similar to those of the stoichiometric $\text{RuO}_2(110)$ surface without on-top oxygen.¹⁹

In a second TPR experiment, we determined the CO_2 yields of $m/e = 44$ and $m/e = 46$ for a 0.7 ML precovered on-top ^{18}O surface, i.e., the CO coverage was only 0.3 ML (cf. Figure 3, bottom panel). This situation was close to the experimental conditions in recent HREELS experiments.¹³ On the average, an adsorbed CO molecule was surrounded by two O_{br} and 1.4

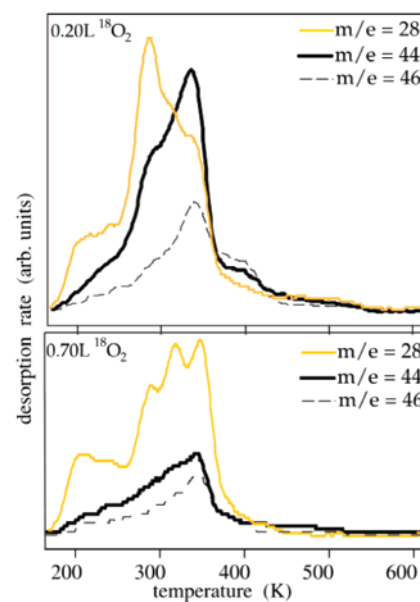


Figure 3. CO_2 spectra for $m/e = 44$ ($^{16}\text{O}^{12}\text{C}^{16}\text{O}$) are compared to those of $m/e = 46$ ($^{16}\text{O}^{12}\text{C}^{18}\text{O}$). The CO molecules, which do not react to form CO_2 , leave the surface via desorption ($m/e = 28$). Upper panel: The $\text{RuO}_2(110)$ surface prepared by $^{16}\text{O}_2$ was first exposed to 0.2 L $^{18}\text{O}_2$ at RT and then saturated by exposing 3 L $^{12}\text{C}^{16}\text{O}$ at 170 K; the O_{ot} coverage corresponds to 0.2 ML. Bottom panel: The $\text{RuO}_2(110)$ surface was first exposed to 0.7 L $^{18}\text{O}_2$ corresponding to an on-top ^{18}O coverage of ca. 0.7 ML and then saturated by CO.

O_{ot} atoms. The TPR measurements indicated that about 1.4 times more CO_2 of $m/e = 44$ ($^{16}\text{O}^{12}\text{C}^{16}\text{O}$) was produced than CO_2 of $m/e = 46$ ($^{16}\text{O}^{12}\text{C}^{18}\text{O}$).

The CO_2 and CO spectra in Figure 3 were corrected for the different sensitivities of the mass spectrometer to CO and CO_2 (including the cracking pattern of CO_2). In this case, the conversion probability was given by the ratio of produced CO_2 and the total amount of CO on the surface before the reaction had started. The overall conversion probability, considering the sum of the $m/e = 44$ and $m/e = 46$ signals, was 40% for the 0.7 ML precovered on-top ^{18}O surface and therefore significantly lower than that for the 0.2 ML precovered surface (65%).

It should be noted that for $^{18}\text{O}_{\text{ot}}$ precoverages smaller than 0.2 to 0.3 ML, no oxygen desorbed in the temperature range 300–500 K, and thus all O_{ot} atoms were consumed. However, if the $^{18}\text{O}_{\text{ot}}$ precoverage exceeded 0.3 ML, oxygen desorbed partly with a maximum rate at 430 K.

In Figure 4, we summarize the CO_2 yields of $m/e = 46$ ($^{16}\text{O}^{12}\text{C}^{18}\text{O}$) for varying on-top ^{18}O precoverages. In determining the CO_2 yield, we integrated the CO_2 TD traces of $m/e = 46$ from 170 to 600 K (cf. Figure 3). The helmet-like shape of the normalized CO_2 yield exhibits a maximum at 0.2 to 0.3 ML.

For comparison, we show in Figure 5 the total CO_2 yield ($m/e = 44$) as a function of the O_{ot} precoverage. These data were extracted from another experiment, where exclusively $^{16}\text{O}_2$ was used to produce the various O_{ot} precoverages. The strictly linear relationship between O_{ot} precoverage and the CO_2 yield of $m/e = 44$ suggested that the CO_2 yield depends solely on the total CO coverage accommodated at the surface. The CO coverage (upper axis in Figure 5) is given by $(1-\theta)$, with θ being the coverage of O_{ot} . The CO_2 yield was normalized to the maximum CO_2 yield of the bare $\text{RuO}_2(110)$ surface, when no on-top oxygen was present and the surface was saturated by CO.

(18) Schaub, R.; Wahlström, E.; Rønnow, A.; Lægsgaard, E.; Steensgaard, I.; Besenbacher, F. *Science* **2003**, *299*, 377.

(19) Wendt, S.; Seitsonen, A. P.; Kim, Y. D.; Knapp, M.; Idriss, H.; Over, H. *Surf. Sci.* **2002**, *505*, 137.

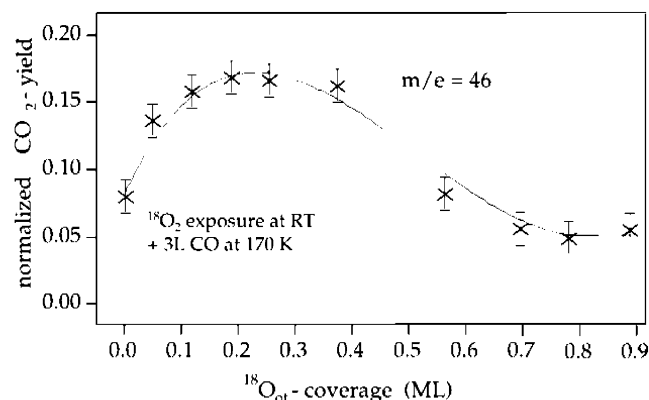


Figure 4. The $^{16}\text{O}^{12}\text{C}^{18}\text{O}$ ($m/e = 46$) yield (integrated from 170 to 600 K) from an $^{18}\text{O}_{\text{ot}}$ precovered $\text{RuO}_2(110)$ surface is shown as a function of the on-top ^{18}O precoverage. The CO_2 yield was normalized to the maximum CO_2 yield of the bare $\text{RuO}_2(110)$ surface.

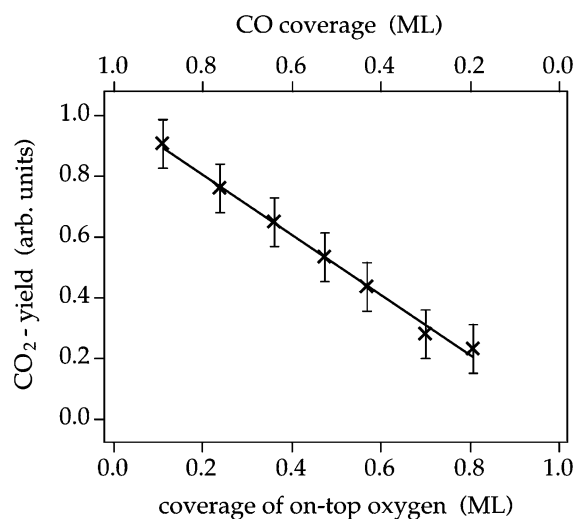


Figure 5. The total CO_2 yield from $\text{RuO}_2(110)$ surface as a function of the on-top ^{16}O coverage. The stoichiometric $\text{RuO}_2(110)$ surface was precovered with various amounts of on-top ^{16}O oxygen and subsequently saturated with CO. The total CO_2 yield was determined by integrating the CO_2 and CO signals over the temperature region of 170–600 K.

4. Discussion

In section 3.1 we demonstrated that O_{ot} and O_{br} atoms on $\text{RuO}_2(110)$ did not exchange appreciably below a surface temperature of 350 K. Since coadsorbed CO does not affect the binding energies of on-top O and bridging O by more than 0.1 eV (according to DFT calculations by Seitsonen in ref 20), we do not expect a significant change of the exchange ratio by the presence of coadsorbed CO. The reaction of adsorbed CO and surface oxygen, however, is almost completed at 350 K (cf. Figure 3). Therefore, we can safely assume for the following discussion that the $m/e = 44$ and $m/e = 46$ CO_2 TPR spectra are associated with the recombination of CO with $^{16}\text{O}_{\text{br}}$ and $^{18}\text{O}_{\text{ot}}$, respectively.

Our temperature-programmed reaction experiments in section 3.2 provide strong evidence that the O_{ot} and O_{br} atoms are comparably active in the oxidation of adsorbed CO molecules.

In estimating the recombination probabilities of CO with O_{ot} and O_{br} from Figure 3, we have to take into account that the experimentally observed reaction rates are proportional to the coverages of the reacting species. Considering also that the uncertainty of the on-top coverage is about 0.1 ML, the rate constants (or recombination probability) of CO with O_{ot} and O_{br} are virtually identical. Similar recombination probabilities of CO with O_{ot} and O_{br} are also supported by the identical shape of the CO_2 TPR traces ($m/e = 44$ and $m/e = 46$) in Figure 3. Therefore, the rate-determining step in both recombination processes is suggested to be equal.

The CO_2 yield ($m/e = 46$) versus $^{18}\text{O}_{\text{ot}}$ precoverage in Figure 4 is also consistent with similar recombination probabilities of CO with O_{ot} and O_{br} atoms. If CO molecules recombine only with O_{ot} , we expect to find a maximum at 0.5 ML in a simple mean field approach, i.e., $(1-\theta)\theta$ dependence with θ being the on-top ^{18}O coverage and $(1-\theta)$ being the on-top CO coverage. However, when the CO molecules recombine also with O_{br} atoms, the maximum will be shifted to lower on-top O coverages consistent with a maximum around 0.2 ML in Figure 4.

Altogether, the presented experimental reaction data are consistent with O_{ot} being similarly active as O_{br} . This conclusion is unexpected in terms of the BEP relationship. According to the BEP-type relationship,¹² the activation energy and the energy change of a given reaction are linearly related, i.e., the greater the thermodynamic driving force for a reaction the lower its barrier will be. Such a BEP relationship has been found to hold for a number of reactions using state-of-the-art density functional theory (DFT) calculations.^{21,22} Since the O_{ot} species is weaker bound by 1.4 eV than O_{br} atoms on $\text{RuO}_2(110)$, the BEP relationship predicts that the on-top species is much more efficient in the oxidation of CO than O_{br} atoms.

The strongest argument against the expected catalytic dominance of the O_{ot} in the CO oxidation reaction on $\text{RuO}_2(110)$ comes from the experiments summarized in Figure 5. In this case, the O_{ot} species was also ^{16}O . If the CO oxidation reaction were dominated by the weakly bound on-top O species, then we would expect to find a parabolic behavior of the CO_2 yield as a function of the on-top O coverage and a maximum of the CO_2 yield at 0.5 ML. However, in Figure 5, a strictly linear dependence is seen.

The HREELS data can be equally explained when CO reacts with similar efficiency with O_{ot} and O_{br} . Fan et al.¹³ observed a disappearance of the O_{ot} signal upon CO exposure at 300 K, preceding the decrease in the O_{br} signal. This observation in HREELS was taken as evidence for the dominating activity of O_{ot} in the CO oxidation reaction. However, this experimental finding does not exclude a recombination of O_{br} with CO. The recombination of CO and O_{br} creates vacancies in the O_{br} rows. These vacancies are rapidly repopulated by the diffusion of O_{ot} into such vacancies. From a thermodynamical viewpoint, this diffusion process is highly favorable since the oxygen atoms thereby gain 1.4 eV in adsorption energy.²⁰ Additionally, this replenishing process is not kinetically hindered due to a diffusion barrier of only 0.7 eV for O_{ot} to migrate into an adjacent

(20) Seitsonen, A. P.; Over, H. Ruthenium Dioxide, a Versatile Oxidation Catalyst: First Principles Analysis. In *High Performance Computing in Science and Engineering, Munich 2002*, Transactions of the first joint HLRB and KONWIHR status and result workshop, Technical University of Munich, Germany, Oct 10–11, 2002; Wagner, S., Hanke, W., Bode, A., Durst, F., Eds.; Springer-Verlag: Berlin, 2003; p 177.

(21) Pallassana, V.; Neurock, M. *J. Catal.* **2000**, *191*, 301.

(22) (a) Nørskov, J. N.; Bligaard, T.; Logadottir, A.; Bahn, S.; Hansen, L. B.; Bollinger, M.; Bengaard, H.; Hammer, B.; Slijvančanin, Z.; Mavrikakis, M.; Xu, Y.; Dahl, S.; Jacobsen, C. J. H. *J. Catal.* **2002**, *209*, 275. (b) Michaelides, A.; Liu, Z. P.; Zhang, C. J.; Alavi, A.; King, D. A.; Hu, P. *J. Am. Chem. Soc.* **2003**, *125*, 3704.

O-bridge vacancy.²⁰ Therefore, the overall effect of CO molecules that recombine with both O_{br} and O_{ot} atoms is a depletion of the O_{ot} coverage, and only after all O_{ot} atoms have been consumed does the concentration of O_{br} atoms start to reduce, as seen in HREELS. It would be helpful to study with HREELS the CO oxidation reaction under steady-state conditions offering $^{18}O_2$ and CO. Under such conditions, we expect that the O_{br} positions are gradually replaced by ^{18}O .

Fan et al. also considered the possibility for the CO oxidation reaction with O_{br} atoms and the subsequent migration of O_{ot} into O_{br} vacancies.¹³ However, this reaction sequence was dismissed on the basis of CO coadsorption experiments using $^{18}O_2$ and $^{16}O_2$, respectively, for populating the on-top O species first. Fan et al. argued that the missing isotope shift for the O_{br} loss by 2.5 meV excludes the ^{18}O atoms to be on bridge positions. Following our interpretation that O_{ot} and O_{br} are similarly active in the CO oxidation reaction, we do not expect a strong isotope shift under the experimental conditions in ref 13. Only a small fraction of the O_{br} atoms is replaced by ^{18}O via migration from O_{ot} into the bridging O vacancies the other bridging O atoms are still ^{16}O .

5. Conclusion

The CO oxidation on $RuO_2(110)$ is a surprisingly rich and complex reaction. On the oxygen-enriched $RuO_2(110)$ surface, two reaction pathways are conceivable: the recombination of CO with on-top O and bridging O. Below 350 K, an exchange of O_{ot} and O_{br} can safely be ruled out. Our TPR experiments indicate that the weakly bound on-top O species is as active as the O_{br} atoms on $RuO_2(110)$ in oxidizing CO, although the on-top O species is much less strongly bound than O_{br} atoms (by 1.4 eV). This surprising finding violates the well-known Brønsted–Evans–Polanyi relationship¹² in catalysis. We argue that the on-top oxygen species is predominantly used to replenish the O_{br} vacancies.

Acknowledgment. We thank A.P. Seitsonen for stimulating and fruitful discussions. Part of the project was supported by the Deutsche Forschungsgemeinschaft via the Contract Ov21/4.

JA0364423